Supporting Information

Haanstra *et al.* 10.1073/pnas.0806664105

SI Text

Extent of Mislocalization Varies Between Enzymes. Previous studies on the role of PEX14 in protein import reported on the localization of only a few representative glycosomal enzymes (1, 2). Those data showed that for the proteins examined there was a shift toward cytosolic localization in the PEX14 mutant, but also suggested that a fraction of some enzymes may still be glycosomal. For the present study, however, the localization of *all* glycolytic enzymes is relevant, particularly given the difference between the model predictions and the measured concentrations of Fru6P and Fru1,6BP (see Fig. S2). According to the model calculations of Fig. 2 and Fig. S2, the accumulation of hexose phosphates should occur when the activities of all glycolytic enzymes reside in the cytosol. It should also occur when a fraction of each glycolytic enzyme would be relocalized to the cytosol. The persistence of a parallel glycosomal route that functions properly should not disturb this. However, if e.g., more aldolase (ALD) were to relocalize to the cytosol than phosphofructokinase (PFK), this might prevent accumulation of Fru1,6BP.

To study the cellular location of the glycolytic enzymes, we differentially disrupted plasma and organellar membranes with increasing concentrations of digitonin and monitored the supernatant fractions by Western blot analysis (Fig. S3*A*). Low concentrations of digitonin permeabilize the plasma membrane, whereas higher concentrations also disrupt glycosomal membranes. Phosphoglycerate kinase (PGK), which is mainly cytosolic in the insect stage (3), was released at low digitonin concentrations (0.05 mg·mL^{-1}) in the induced (+Tet) and in the uninduced (−Tet) cells. Glucose-6-phosphate isomerase (PGI) and ALD, both glycosomal proteins, were only released at higher digitonin concentrations in the uninduced (-Tet) cells, consistent with a glycosomal localization. In agreement with earlier observations (2), the PEX14-depleted cells released some, but not all ALD at lower digitonin concentrations than uninduced cells. This suggests that only a small fraction of ALD was cytosolically localized in the induced mutant, with a large part still inside glycosomes. In contrast, substantially more mislocalization of PGI occurred in the cells induced for PEX14 RNAi, with most released at 0.05 mg·mL^{-1} of digitonin and no additional PGI release at the higher concentrations. For a more quantitative picture of the mislocalization of functional enzymes, we also measured enzyme activities (V_{max}) in digitonin fractions (Fig. S3*B*). In the uninduced cells, as expected, activities corresponding to the first steps of glycolysis [from hexokinase (HXK) to ALD] were released only at high digitonin concentrations. In PEX14-depleted cells, PGI activity was clearly mislocalized with 80% of the activity released at 0.1 mg·mL^{-1} digitonin, similar to the Western blot results (Fig. S3*A*). There was no large difference in the patterns observed for HXK, PFK and ALD between induced and uninduced cells, but at low concentrations of digitonin there was a detectable release of these enzymes from the induced cells. Glyceraldehyde-3-phosphate dehydrogenase (GAPDH) activity was not measured since both a cytosolic and glycosomal isoform are normally expressed (4). Together, the Western blots and enzyme activities show that not all enzymes of the upper part of glycolysis were mislocalized to the same extent in PEX14-deficient cells, with PGI showing by far the most mislocalization. In the extreme case that a fraction of the glycosomes contains little or no PGI at all, this could result in a glycosomal pathway that is effectively truncated at the level of Glc6P. This scenario provides an alternative explanation for the accumulation of Glc6P in the induced cells without the accumulation of Fru6P or Fru1,6BP.

Northern Blot Analysis of the PEX14 and Glycerol Kinase Single and Double RNAi Mutants. Tetracycline (Tet) was added to induce RNAi, and samples for Northern blot analysis were taken after 2 days to determine whether glycerol kinase (GK) and PEX14 transcript levels were reduced in the appropriate cell lines. Upon induction of RNAi, both the GK and PEX14-GK RNAi lines showed a significant reduction in GK mRNA levels (Fig. S4*A*). By contrast, the levels of PEX14 mRNA are unchanged in the GK RNAi mutant. Similarly, both the PEX14 and PEX14/GK RNAi mutants showed strong reductions in the abundance of PEX14 transcripts upon induction, whereas the GK RNAi line did not (Fig. S4*B*). In the PEX14 blot, the PEX14 endogenous transcript is degraded and some double stranded RNA generated from the RNAi construct is visible (this is larger for the PEX14-GK line because the RNAi construct has fragments of both genes). Degradation fragments are seen near the bottom of the blot.

Comparison of 2 Independently Constructed PEX14-RNAi Cell Lines. The experiments described in the main text were done on the PEX14-RNAi mutant that was constructed in cell line PF 29–13 (1). These experiments were repeated in a PEX14-RNAi mutant that was constructed from cell line PF 449 (2). The results obtained with the latter strain are shown here.

Specific Enzyme Activities. We measured the specific enzyme activities of 9 glycosomal enzymes in supernatants of digitonin-treated cells of both PEX14-RNAi cell lines in the absence of tetracycline (Table S1). Without induction of RNAi, the PEX14-RNAi cell line for which the results are described in the main text, has a markedly higher activity of HXK.

Enzyme Localization. The localization experiments displayed in Fig. 4 of the main text and Fig. S3*B* (PF 29–13-PEX14 RNAi) were also done on the PF449-PEX14 RNAi mutant (Fig. S6). The results for both mutated cell lines are similar.

Metabolite Profile. Glucose and glycerol pulses of 25 mM were given to uninduced and induced cultures of the PF449-PEX14 RNAi mutant (Fig. S7). The results for the PF 29–13-PEX14 RNAi cell line are respectively displayed in Fig. 2 *Right*, Fig. S2 *Right*, and Fig. 3*B*.

In contrast to the induced PF 29–13-PEX14 RNAi cell line (main text), the PEX14 RNAi mutant made in PF449 did not accumulate Glu6P when given a glucose pulse, but moderately accumulated Gly3P upon a glycerol pulse.

mRNA Levels for PEX14. Changes in mRNA levels of PEX14 were followed in time in uninduced and tetracycline-induced cells of both cell lines by quantitative PCR (Fig. S8). There was no difference between the changes in mRNA levels in the 2 lines.

SI Material and Methods

Details of Changes to Metabolite Measurement Protocols as Described in Main Text. For Glc6P and Fru6P the reaction mixture contains: 63 mM triethanolamine (TEA), pH 7.6, 0.63 mM $NADP^+$, 6.3 mM $MgSO_4$, 1.2 units·mL^{-1} glucose-6-phosphate dehydroge-

nase (G6PDH) (Sigma) and for Fru6P also 2.5 units·mL PGI. For Fru1,6BP: 60 mM TEA, pH 7.6, 0.14 mM NADH, 1.1 units·mL^{-1} glycerol-3-phosphate dehydrogenase (G3PDH) (Sigma), 4.3 units·mL^{-1} triosephosphate isomerase (TIM) (Roche) and 0.15 units·mL^{-1} ALD (Roche). Gly3P was measured according to ref. 5, in a reaction mixture with 0.13M glycine/0.63M hydrazine, 1.1 mM NAD^+, 1.3 mM ATP and 0.95 mM $MgSO_4$ and 1.1 units·mL^{-1} G3PDH.

Northern Blot Analysis. RNA was obtained by extracting 5×10^7 parasites with TRIzol reagent (Invitrogen). Approximately 10 μg of RNA was loaded onto formaldehyde/agarose gels for electrophoresis. After transfer to Nytran nylon membranes (Schleicher and Schuell), blots were placed in ULTRAhyb (Ambion) and probed with the antisense RNA probe corresponding to the RNAi fragments described above according to the manufacturer's recommendations.

Fractionation by Digitonin Titration for Western Blot Analysis. For Western blot analysis, fractionation with digitonin was carried out as described in ref. 2. A sample treated with 0.1% Triton X-100 was taken as a reference for complete release of all cytosolic and glycosomal protein content. After fractionation, supernatant was collected for Western blot analysis and stored at −80°C in Laemmli buffer (6).

Fractions were heated for 5–10 min at 95°C and their proteins separated by SDS/PAGE (12.5% acrylamide) and transferred to a methanol-activated PVDF-membrane (BioRad) and blocked for 1 h in 5% nonfat milk powder in TBST [Tris·HCl 20 mM, NaCl 136 mM, pH 7.5 with 0.05% (vol/vol) Tween 80]. After washing in TBST, anti-TbPGK (1:150,000), anti-TbALD (1:200,000) and anti-TbPGI (1:50,000) were used as primary antisera. HRP-linked anti-rabbit IgG (DAKO) (1:2000) was used as a secondary antibody and HRP activity was measured after 2 min incubation with Lumi-Light^{PLUS} Western blot analysis substrate (Roche).

Quantitative PCR. Amplification, data collection and data analysis were done in the ABI 7700 Prism Sequence Detector (2 min at 50°C; 10 min at 95°C; and 40 cycles of 15 s at 95°C followed by 1 min at 59°C). The calculated cycles of threshold values (Ct) were exported to Microsoft Excel and analyzed further. Cycles of threshold for the different genes were normalized by subtracting the Ct of hypoxanthine-guanine phosphoribosyl transferase transcript in the same sample (ΔCt). A different housekeeping gene (ß-tubulin) was assayed as an internal standard. Subsequently the normalized Ct values of the different time points were, for each transcript, compared with the Ct of that transcript at time point zero to calculate the fold changes of the mRNA concentrations according to: $\mathrm{mRNA}(t)/\mathrm{mRNA}(0) = 2^{(\Delta\mathrm{Ct}(0) - \Delta\mathrm{Ct}(t))}$.

1. Furuya T, Kessler P, Jardim A, Schnaufer A, Crudder C, Parsons M (2002) Glucose is toxic to glycosome-deficient trypanosomes. *Proc Natl Acad Sci USA* 99:14177–14182.
2. Moyersoen J, *et al.* (2003) Characterization of *Trypanosoma brucei* PEX14 and its role in the import of glycosomal matrix proteins. *Eur J Biochem* 270:2059–2067.
3. Hart DT, Misset O, Edwards SW, Opperdoes FR (1984) A comparison of the glycosomes (microbodies) isolated from Trypanosoma brucei bloodstream form and cultured procyclic trypomastigotes. *Mol Biochem Parasitol* 12:25–35.
4. Misset O, Opperdoes FR (1987) The phosphoglycerate kinases from. *Trypanosoma brucei Eur* J Biochem 162:493–500.
5. Bergmeyer HU (1974) *Methods of enzymatic analysis* (Academic, New York).
6. Laemmli UK (1970) Cleavage of structural proteins during the assembly of the head of bacteriophage T4. *Nature* 227:680–685.

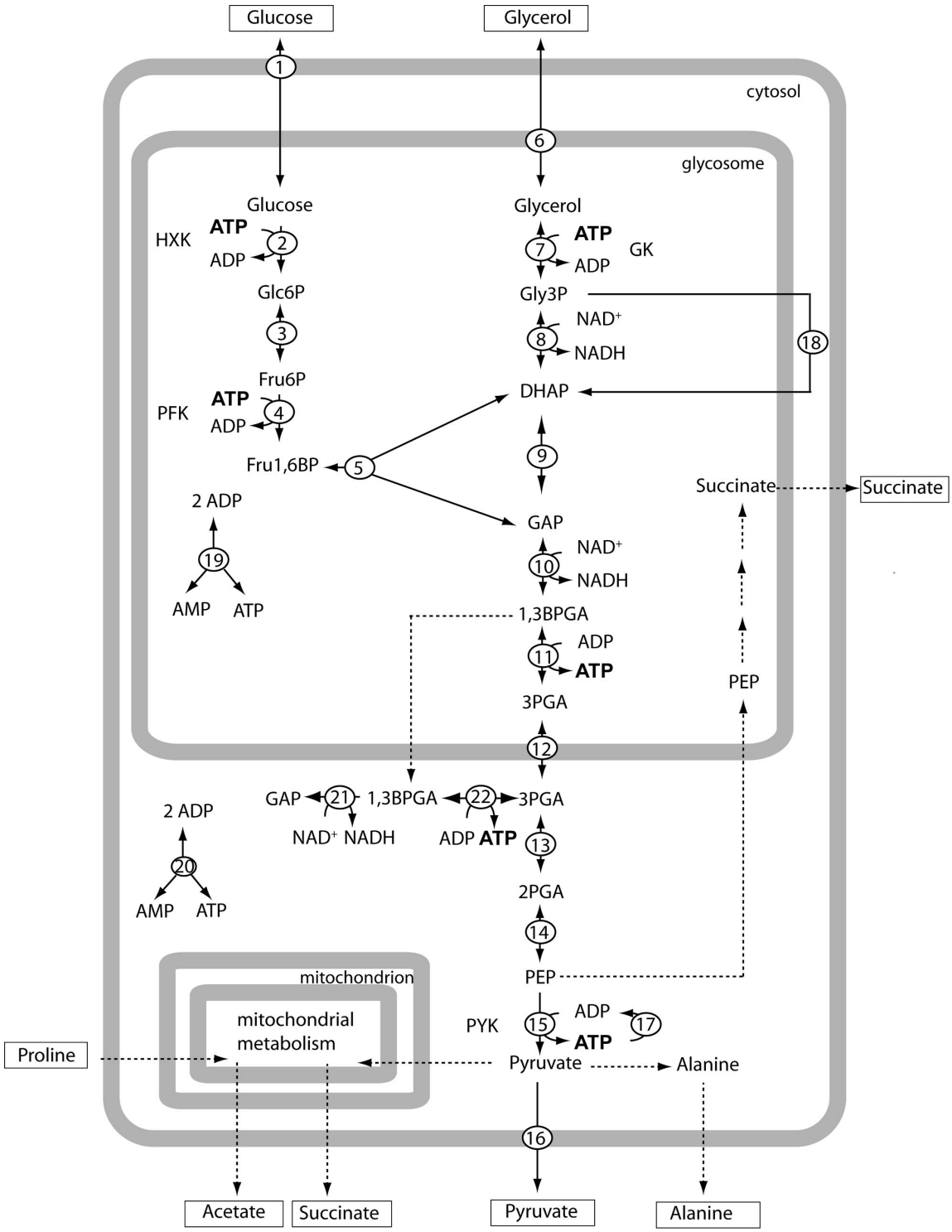

Fig. S1. Glycolysis of *T. brucei*. Detailed scheme of glycolysis in *T. brucei*. 1: glucose transport over plasma membrane and glycosomal membrane; 2: HXK; 3: PGI; 4: PFK; 5: ALD; 6: glycerol transport over plasma membrane and the glycosomal membrane; 7: GK; 8: G3PDH; 9: TIM; 10: GAPDH; 11: PGKC; 12: transport of 3PGA over the glycosomal membrane; 13: PGAM; 14: ENO; 15: PYK; 16: pyruvate transport; 17: ATP utilization; 18: AOX (mitochondrial); 19: glycosomal adenylate kinase; 20: cytosolic adenylate kinase; 21: cytosolic GAPDH; 22: PGKB. Solid lines represent reactions in bloodstream form and procyclic metabolism, dashed lines are exclusively procyclic. In procyclic forms, in contrast to bloodstream forms, there is limited glycosomal PGK activity (reaction 11) and PGK is mainly cytosolic (reaction 22). In the computer model, only the bloodstream form reactions are included. Reactions 6, 12, 19 and 20 were modeled as equilibrium reactions.

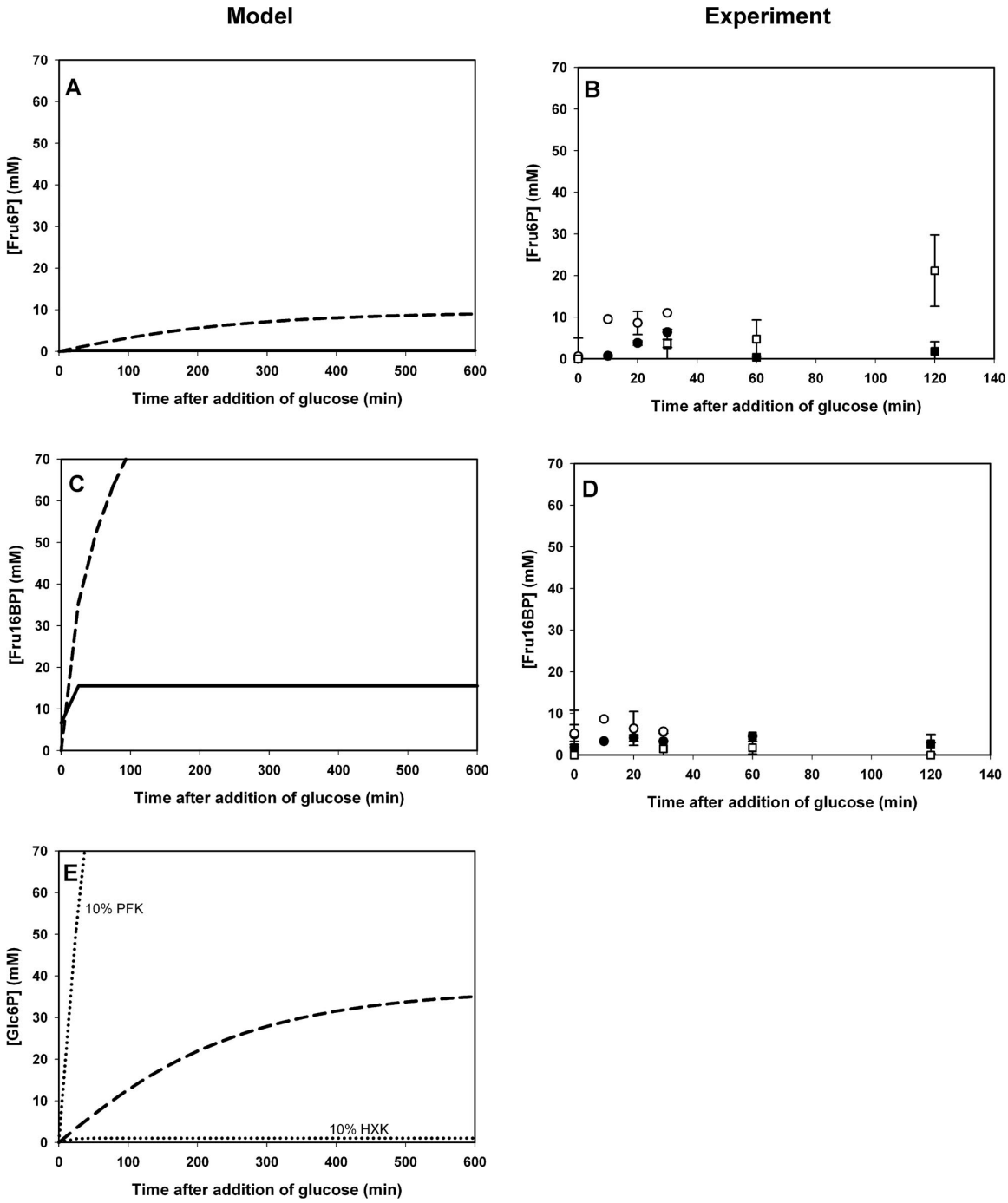

Fig. S2. Metabolite profiles in the model and in experiments after the addition of glucose. Glucose (25 mM) was added at t = 0 in the models and in experiments. (*Left*) Model systems. Calculated concentrations of Fru6P (*A*) and Fru1,6BP (*C*) in time, in the model with (solid line) or without (dashed line) the glycosome. (*E*) Calculated concentration of Glc6P in the model without a glycosome at normal total cellular levels of HXK and PFK (dashed line), and when HXK or PFK levels were decreased to 10% of their original levels (dotted lines). When the activity of HXK was down-regulated to 10% of its wild-type level, the glycosome-deficient model did not accumulate Glc6P anymore. In contrast, down-regulation of PFK even enhanced accumulation of Glc6P, consistent with the fact that the latter is a substrate for PFK. Both observations are in agreement with previously published experiments that HXK-RNAi rescued the PEX14 mutant, whereas PFK-RNAi did not [Kessler PS, Parsons M (2005) Probing the role of compartmentation of glycolysis in procyclic form *Trypanosoma brucei*: RNA interference studies of PEX14, hexokinase, and phosphofructokinase. *J Biol Chem* 280:9030–9036]. (*Right*) Experiments. Intracellular concentrations of Fru6P (*B*) and Fru1,6BP (*D*) were measured in time in PEX14-RNAi cultures. Filled symbols, uninduced cultures; open symbols, Tet-induced cultures. Squares and circles represent biological replicates. Error bars represent standard deviations of 2 measurements in the same sample.

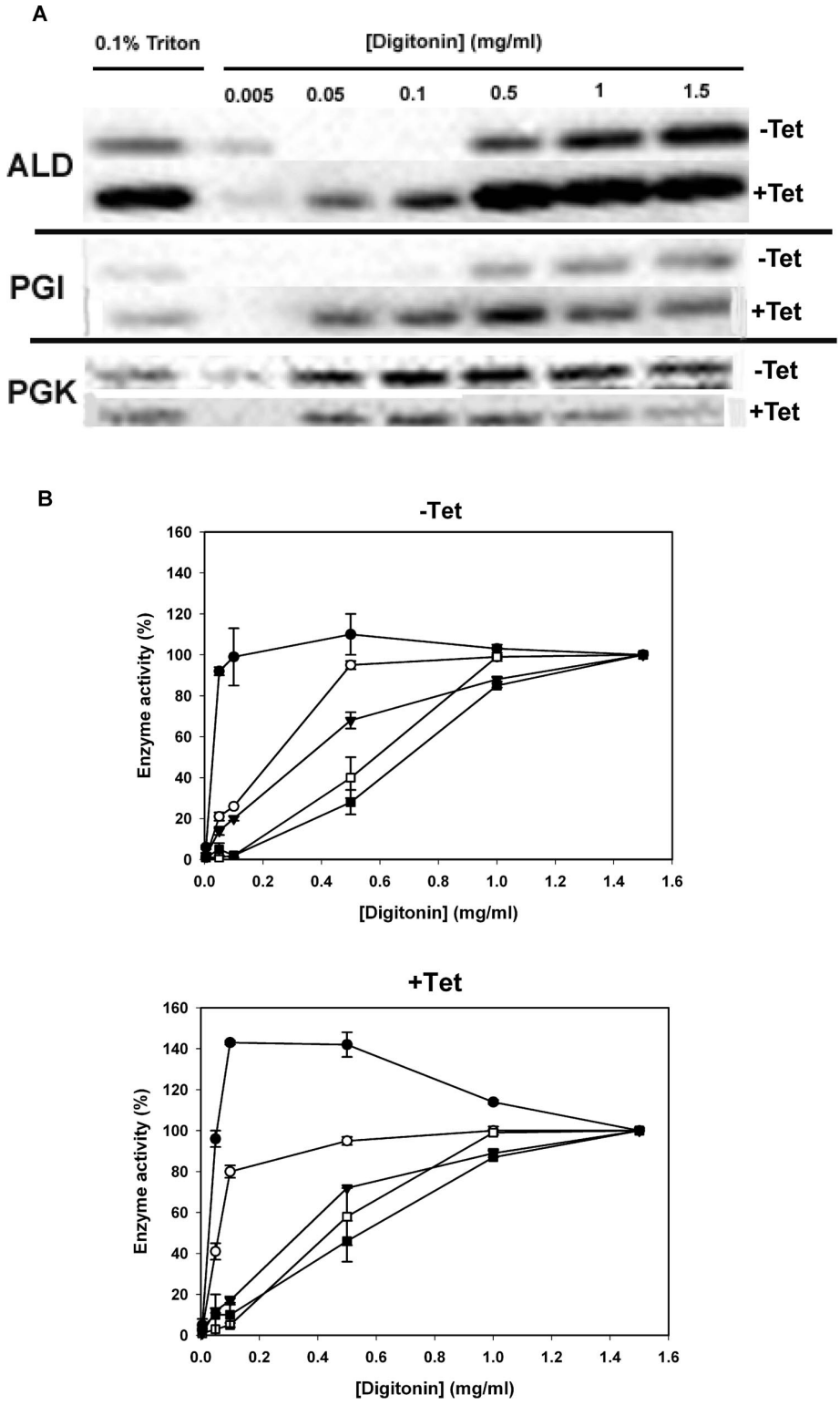

Fig. S3. Subcellular localization of the enzymes in the upper part of the glycolytic pathway. Pex14-RNAi cells were permeabilized by different concentrations of digitonin and enzyme concentrations and activities were measured in the supernatant. PGK was used as a cytosolic control. (*A*) Western blot of supernatants from permeabilized cells uninduced (−Tet) or induced (+Tet) for RNAi. The specific antisera used are indicated at *Left*. Triton (0.1%) was used as a control for complete release of protein. (*B*) Enzyme activities in the supernatants. (*Top*) Results for uninduced cells (−Tet). (*Bottom*) Results for induced cells (+Tet). In each culture the enzyme activities released at 1.5 milligrams of digitonin per milliliter were taken as 100%. Error bars represent standard deviations of 2 independent biological replicates. Open squares, HK; open circles, PGI; inverted triangles, PFK; filled squares, ALD; filled circles, PGK. See *SI Text* for details.

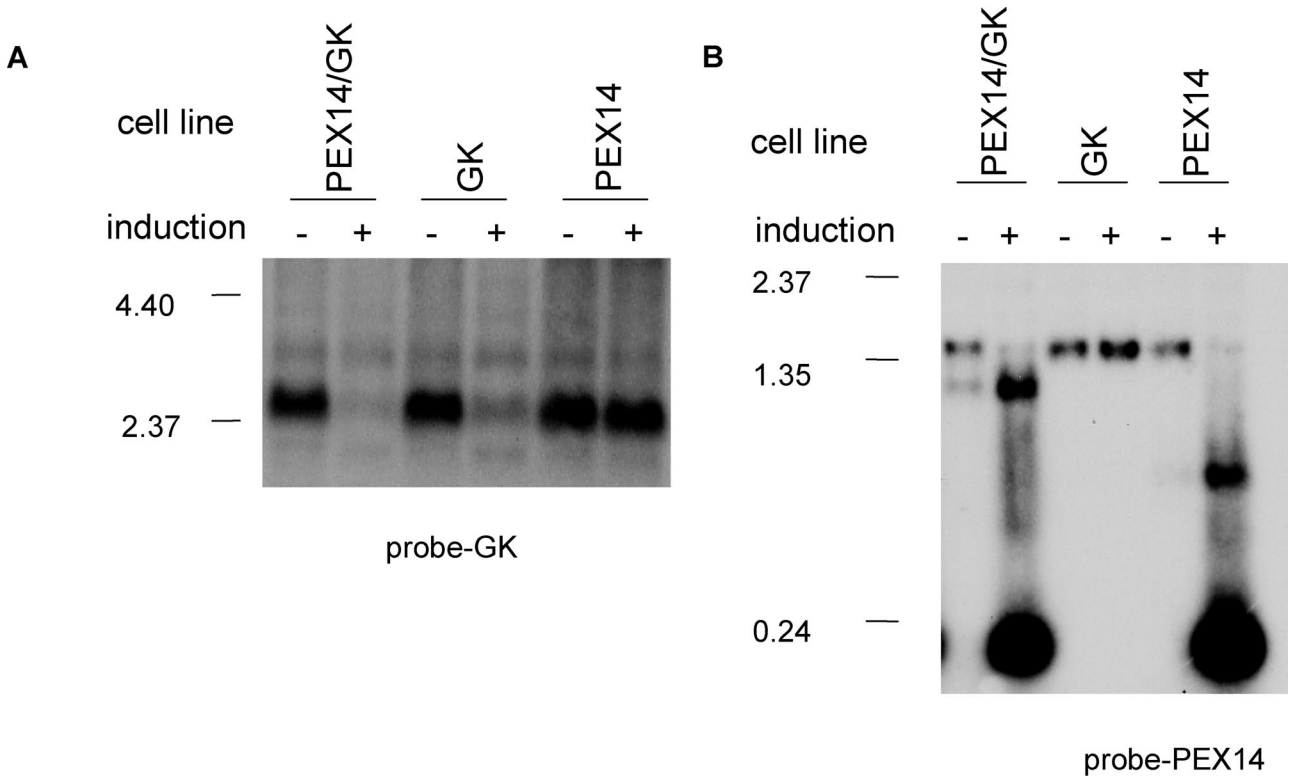

Fig. S4. Northern blot analysis of the PEX14-, GK-, and PEX14-GK RNAi mutants (background PF cell line 29–13). (*A*) GK-probe. (*B*) PEX14-probe. The cells were induced with Tet for 2 days and compared with uninduced cells. RNA was extracted from 5×10^7 parasites with TRIzol reagent (Invitrogen). Approximately 10 μg of RNA was loaded onto formaldehyde/agarose gels for electrophoresis. After transfer to Nytran nylon membranes (Schleicher and Schuell), blots were placed in ULTRAhyb (Ambion) and probed with the antisense RNA probe corresponding to the RNAi fragments described in the text according to the manufacturer's recommendations. See *SI Text* for details.

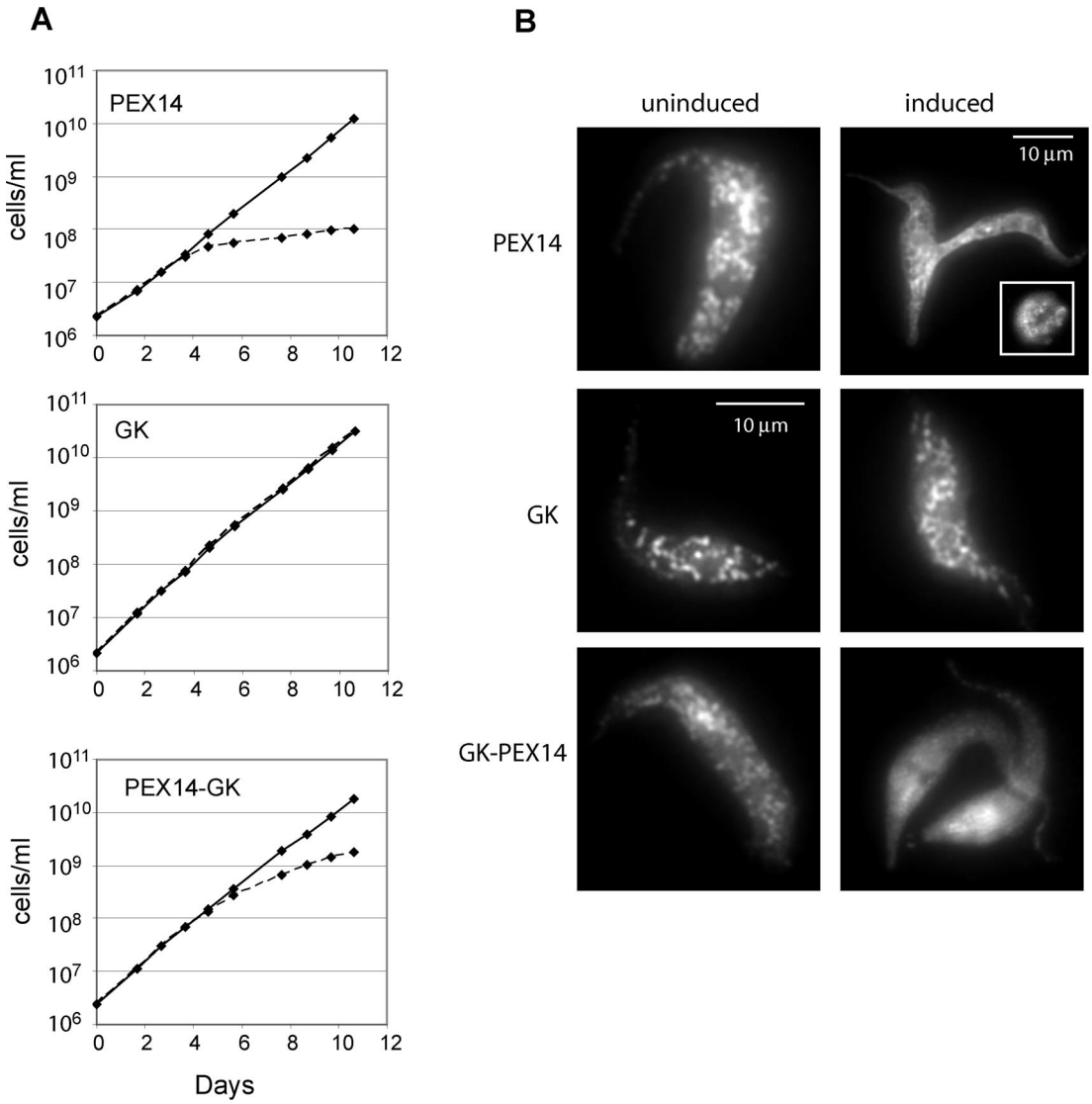

Fig. S5. Knockdown of GK partially rescues the PEX14-depletion phenotype on glucose. (*A*) Cumulative growth of inducible RNAi cells on standard medium (containing 10 mM glucose but no glycerol). Solid lines show uninduced cells and dashed lines show Tet-induced cells (*B*) Immunofluorescence with anti-glycosomal antibody on PEX14-RNAi, GK-RNAi and Pex14-GK RNAi cells in the presence (+Tet) or absence (−Tet) of tetracycline in standard medium.

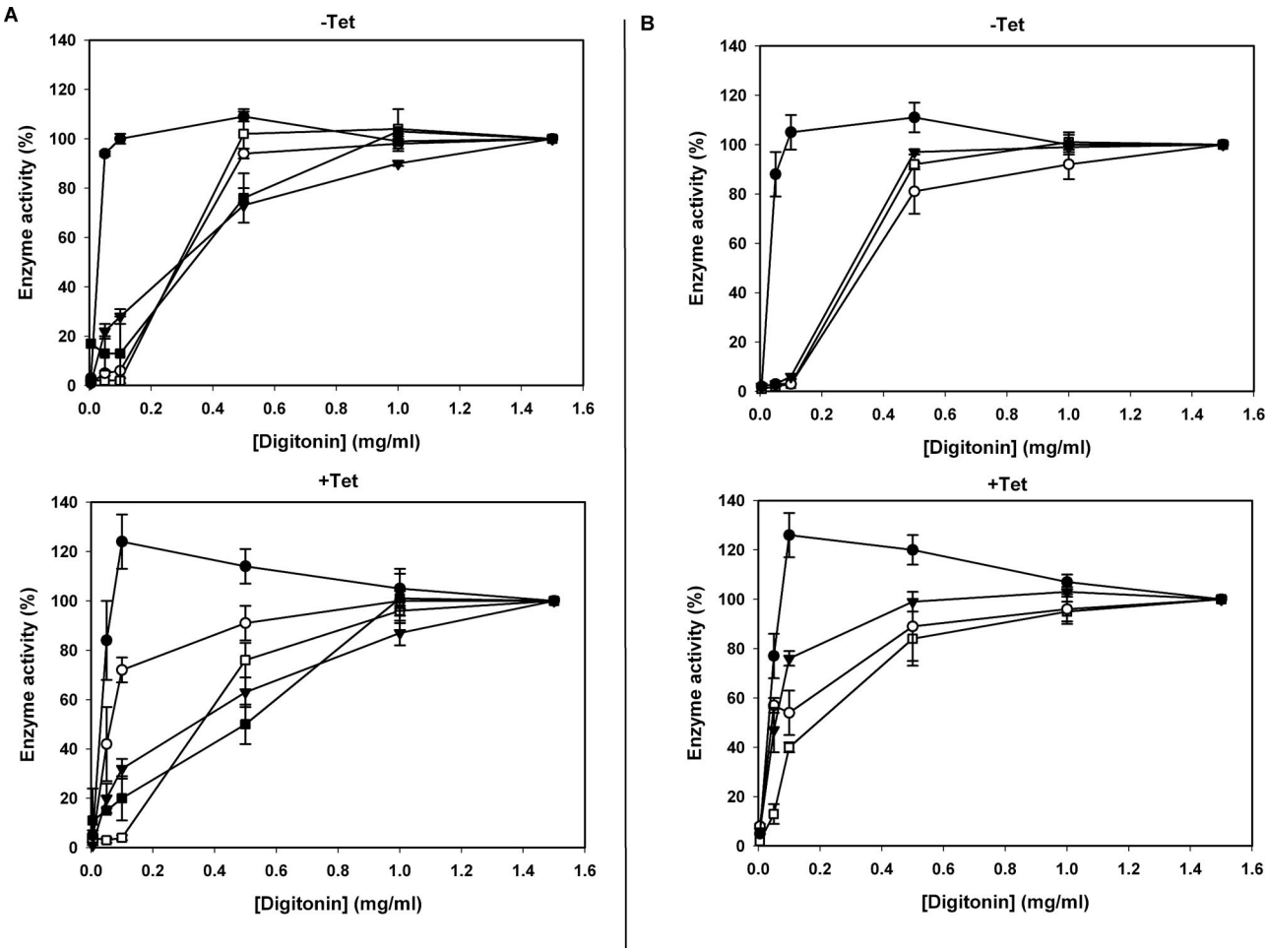

Fig. S6. Enzyme localization in the PF 449 PEX14-RNAi mutant. Cells were permeabilized with different concentrations of digitonin and the supernatant was used for enzyme activity measurements. (*Top*) Results for uninduced (−Tet, DMSO) cells. (*Bottom*) Results for induced cells (+Tet). PGK was used as a cytosolic control. Enzyme activities at [digitonin] = 1.5 mg·mL^{-1} were taken as 100% for each culture. Error bars represent standard deviations of 2 independent experiments. (*A*) Enzyme activities of enzymes of upper glycolysis: open squares, HXK; open circles, PGI; inverted filled triangles, PFK; filled squares ALD; filled circles, PGK (*B*) Enzyme activity of enzymes of the glycerol and pyruvate branch: open squares, GK; open circles, G3PDH; inverted triangles, TIM; filled circles, PGK. See *SI Text* for details.

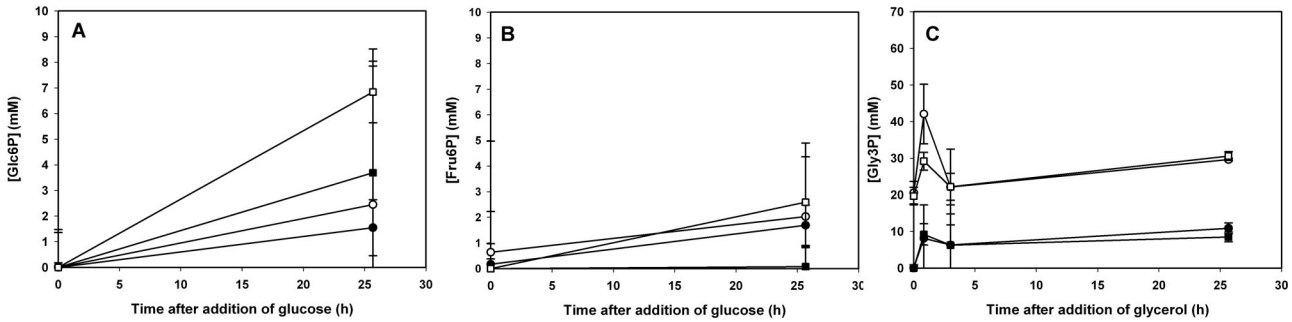

Fig. S7. Metabolite profile of the PF449 PEX14 mutant. At $t = 0$ 25 mM glucose (*A* and *B*) or glycerol (*C*) was given. Closed symbols, uninduced cultures. Open symbols, induced cultures. Squares and circles show independent experiments. Error bars represent standard deviations of 2 measurements of the same sample. Intracellular concentrations are based on total cell counts. See *SI Text* for details.

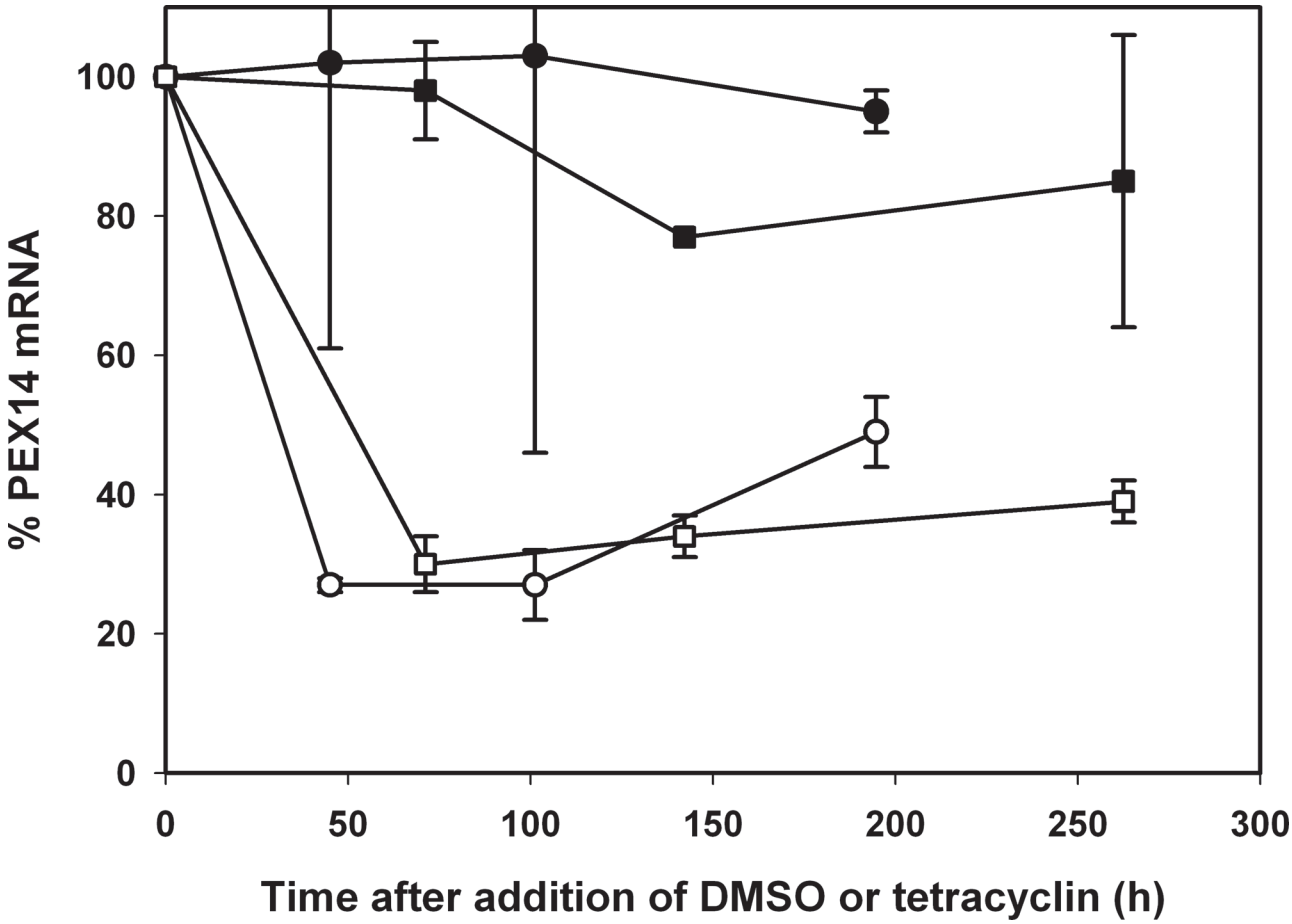

Fig. S8. PEX14 mRNA in PF29–13-PEX14 and PF449-PEX14 RNAi mutant. At t = 0, solvent alone (0.05% DMSO, closed symbols) or 1.0 μg·mL^{-1} tetracycline (open symbols) were added to the cultures. PEX14 mRNA levels at each time point were compared with the levels just before addition of tetracycline or DMSO. Squares, PF29–13-PEX14 (1); circles, PF449-PEX14 (2). Similar results were obtained when 5 μg·mL^{-1} tetracycline was used (data not shown). See *SI Text* for details.

Table S1. Specific enzyme activities in the procyclic form PF 29–13-PEX14 RNAi mutant (results in main text) and the PF 449-PEX14 RNAi mutant (results in Supporting Information 1) and the bloodstream form cell line BF449 (the values that are used in the model)

	Enzyme activity, milliunits/mg protein (*n*)			
Enzyme	PF 29–13-PEX14*	PF 449-PEX14*	Ratio PF 29–13: PF 449	Measured in BF 449†
HXK	12,539 ± 1928 (2)	207 ± 139 (2)	61	1,929 ± 116 (3)
PGI‡	4,345 ± 377 (4)	532 ± 89 (4)	8.2	1,305 ± 115 (3)
PFK	1,363 ± 164 (2)	513 ± 67 (2)	2.7	1,708 ± 299 (3)
ALD	19.8 ± 3.8 (2)	7.2 ± 2.9 (2)	2.8	560 ± 153 (3)
TIM‡	7,485 ± 1947(2)	6,369 ± 1494 (2)	1.2	5,696 ± 294 (3)
G3PDH	252 ± 49 (2)	644 ± 247 (2)	0.39	465 ± 21 (3)
GK‡	7,927 ± 1101 (2)	5,926 ± 1042 (2)	1.3	3,417 ± 143 (3)
PGK‡	581 ± 81 (4)	570 ± 22 (4)	1.0	1,358 ± 254 (3)
PYK	5.66 ± 0.32 (2)	17.6 ± 0.2 (2)	0.32	1,020 ± 221 (3)

PF values were measured at 28°C; BF values were measured at 25°C.

*Measured in cell extracts from uninduced cells, grown on proline and lysed with 1.5 mg·ml^{-1} digitonin.

‡measured in the reverse reaction (forward direction is in the direction of glycerol or pyruvate production; for TIM the forward reaction is from dihydroxyacetone phosphate to glyceraldehyde 3-phosphate).

†Taken from the supplemental data in: Albert M-A, *et al.* (2005) Experimental and in silico analyses of glycolytic flux control in bloodstream form *Trypanosoma brucei. J Biol Chem* 280:28306–28315.